Available online at www.sciencedirect.com
ScienceDirect
Journal of the European Ceramic Society 27 (2007) 1425–1430
www.elsevier.com/locate/jeurceramsoc

Microstructure and mechanical properties of AlN–hBN based machinable ceramics prepared by pressureless sintering

W.S. Cho [a,*], Z.H. Piao [a], K.J. Lee [a], Y.C. Yoo [a], J.H. Lee [b], M.W. Cho [c], Y.C. Hong [d], K. Park [e], W.S. Hwang [a]

[a] School of Materials Science and Engineering, Inha University, Incheon 402-751, Republic of Korea
[b] School of Materials Science and Engineering, Yeungnam University, Gyonsan 712-749, Republic of Korea
[c] School of Mechanical Engineering, Inha University, Incheon 402-751, Republic of Korea
[d] Department of Electronic Engineering, University of Incheon, Incheon 402-749, Republic of Korea
[e] Department of Advanced Materials Engineering, Sejong University, Seoul 143-747, Republic of Korea

Available online 23 June 2006

Abstract

AlN based machinable ceramics containing hBN were prepared by economical pressureless sintering at 1800 °C for 2 h in a nitrogen gas atmosphere. The effects of hBN content on microstructure, mechanical properties and machinability were investigated. The relative density of sintered compacts decreased with increasing hBN content. The four-point flexural strength of 340 MPa for monolithic AlN also decreased to about 120 MPa by the addition of 20 vol% hBN, mainly due to increased porosity. With increasing hBN content, AlN–hBN based ceramic composites revealed increased crack deflection. The Vickers indentation crack paths in specimens were sinusoidal indicating crack bridging and pull-outs of composite grains during crack propagation. During end-milling and microdrilling processes for AlN ceramic composites with more than 10 vol% hBN, measured feed and thrust forces decreased with increasing hBN content, demonstrating a good machinability of the composites.

Keywords: Microstructure; Mechanical properties; Machinable ceramics; Sintering

1. Introduction

Aluminum nitride (AlN) is an excellent candidate for use as substrates in electronic packaging and other electrical and optical applications due to its high thermal conductivity, high translucent properties, and a thermal expansion coefficient close to that of silicon (Si).[1] In order to utilize AlN in precision parts, the focus on machinability becomes paramount. However, the high cutting force and the brittle fracture behavior of this ceramic make it difficult to manufacture complicated shapes for the required application. Although it is possible to machine AlN by diamond abrasives and by laser techniques, these methods have limitations with respect to obtaining complicated shapes and for economical reasons.[2]

It has been known that the addition of hexagonal boron nitride (hBN) improves the machinability of AlN. AlN–BN based ceramics can be machined easily since cleavage plane of h-BN can facilitate crack propagation during machining, thereby decreasing the cutting resistance.[3]

In general, AlN–hBN composite is prepared by hot-pressing since plate-like hBN degrades sinterability. But, it is impossible to manufacture precision parts with complicated shapes by hot-pressing, an expensive sintering method compared with pressureless sintering.

In this paper, we investigated pressureless sintering conditions for AlN ceramics. We also present results of an investigation on the effect of h-BN content on microstructure, mechanical properties and machinability of pressureless-sintered AlN–hBN composites.

2. Experimental

The starting powders were AlN (>99.15% pure, 2.9 μm, Tokuyama Co. Ltd., Japan) and hBN (>99% pure, 6.4 μm, T.D.K. Co. Ltd., Japan). The amounts of hBN added ranged from 0 to 20 vol%. In all specimens, 3 wt% of Y_2O_3 (>99.9% pure, <0.25 μm, Shinestu Chemical Co. Ltd., Japan) was added as sintering aid. The powder mixtures were prepared by wet

* Corresponding author.
E-mail address: wscho@inha.ac.kr (W.S. Cho).

0955-2219/$ – see front matter © 2006 Elsevier Ltd. All rights reserved.
doi:10.1016/j.jeurceramsoc.2006.05.044

ball-milling in ethanol for 72 h in an alumina pot. The mixed wet powders were dried on a hot plate using a rotating stirrer to avoid gravity-induced segregation. The dried and sieved (to 16 mesh) powders were uni-axially pressed into rectangular green compacts (6 mm × 15 mm × 40 mm, forming pressure: 160 MPa) of which the relative density was approximately 50%. Green compacts were pressureless-sintered at 1800 °C for 2 h under the N_2 atmosphere. Rectangular specimens (3 mm × 4 mm × 36 mm) were prepared by cutting, grinding, and polishing of the sintered compact. The density of specimens was measured using the Archimedes method and the theoretical density of the specimens was estimated by the rule of mixture. The relative density, four-point flexural strength, Vickers hardness (load: 98 N, dwell time: 30 s), fracture toughness and Young's modulus were measured. The fracture toughness was measured by indentation fracture (IF) method on surface perpendicular to the forming pressure using a load of 98 N for 30 s.

For the characterization of crack interactions with hBN, Vickers indentations with a load of 98 N were made on the polished surfaces parallel and perpendicular to the direction of the uni-axial forming pressure. In order to evaluate quantitatively the dependence of the degree of crack deflection on BN content, the cumulative length of deflection angles of crack segments to the main crack direction was investigated.

The microstructure of specimens was investigated by SEM and TEM equipped with EDX and XRD. Machinability was evaluated by cutting tests with a WC–Co cutting tool (feed rate: 50, 80, and 100 mm/min, cutting speed: 498 rpm, depth of cut: 0.1 mm), and feed force and thrust force were detected by piezoelectric sensor. Finally, machinability of the composites was evaluated in a microdrilling process (feed rate: 10 mm/min, cutting speed: 4000, 5000, and 6000 rpm, depth of cut: 5 μm). Drills of 100 μm diameter were used for the experiment, and thrust forces were measured using a tool dynamometer under several conditions.

3. Results and discussion

Fig. 1 shows the relative density of specimens with varying content of h-BN. The relative density decreased with increasing h-BN content up to 20 vol%. With 20 vol% addition, the density showed significant decrease to 86.2%. This is the consequence of the role of the plate-like h-BN particles in restricting the rearrangement of AlN particles during sintering.

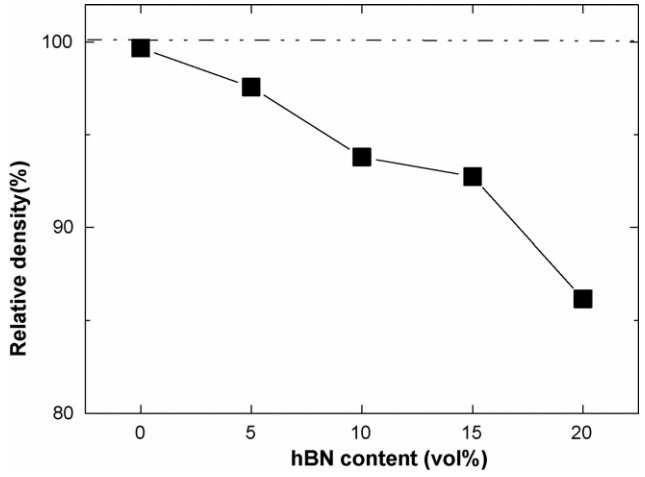

Fig. 1. Effect of hBN content on relative density of AlN–hBN based composites.

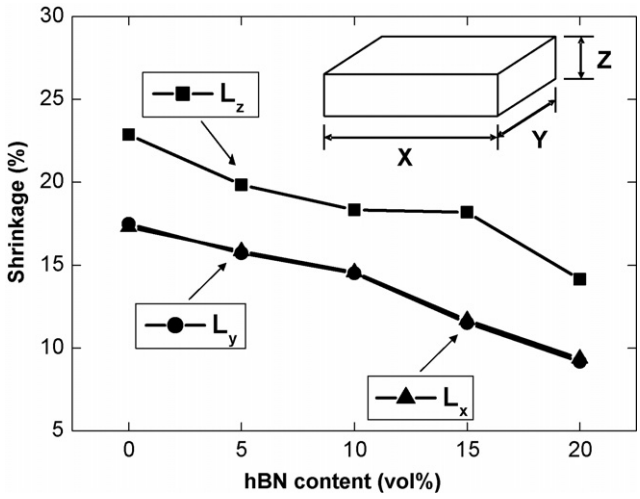

Fig. 2. Shrinkage of AlN–hBN based composites; L_x, L_y and L_z denote linear shrinkage to longitudinal, transverse, and thickness direction of rectangular specimen, respectively.

Fig. 2 presents the effect of h-BN content on the linear shrinkage of AlN. L_x, L_y and L_z in the figure denote linear shrinkages to the longitudinal, transverse, and thickness direction of rectangular specimen, respectively. L_z was parallel to the direction of uni-axial forming pressure. Shrinkages to L_x and L_y directions, perpendicular to the forming pressure, were almost same each other, and showed ~5% lower values than that to the L_z direction. Since hBN platelets in powder mixtures were generally oriented by the uni-axial forming pressure, AlN–hBN green compacts exhibited strong texture of BN grains oriented with the *c*-axis parallel to the forming direction. Thus, the restricting effect of hBN on the rearrangement of AlN particles is expected to be large in perpendicular direction to the forming pressure.

The effect of hBN content on the flexural strength and fracture toughness of AlN is shown in Fig. 3 shows. Both properties decreased with increasing BN content. The flexural

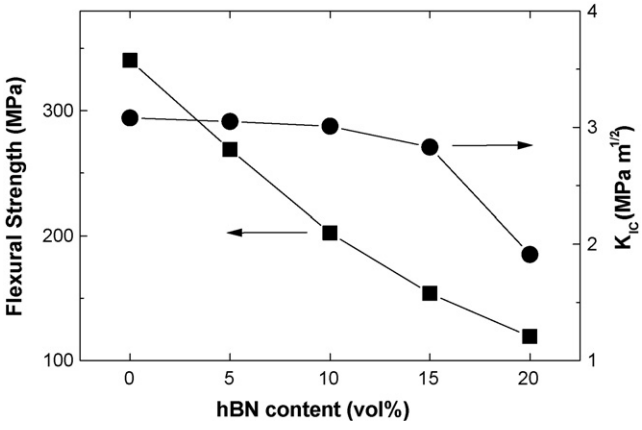

Fig. 3. Effects of hBN content on flexural strength and fracture toughness of AlN–hBN based composites.

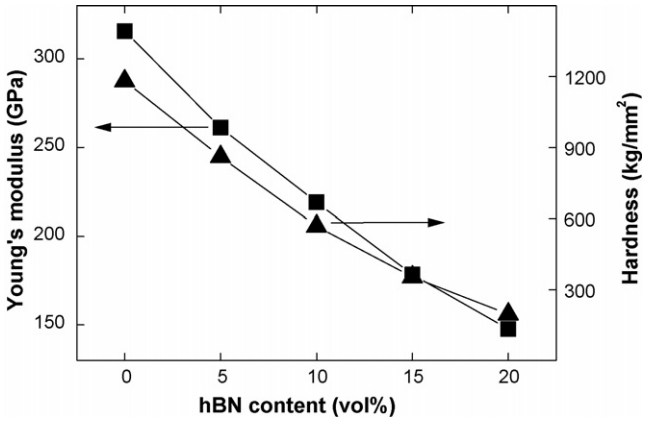

Fig. 4. Effects of hBN content on Young's modulus and hardness of AlN–hBN based composites.

strength decreased by 65%, from 340 MPa for monolithic AlN to 120 MPa for AlN containing 20 vol% hBN. The corresponding decrease in the fracture toughness was about 50%, from 3.1 to 1.9 MPa $m^{1/2}$. In order to investigate the cause for the decrease in strength and fracture toughness resulting from the addition of h-BN, the Young's modulus was measured as a function of h-BN content. The results are shown in Fig. 4 along with the corresponding change in Vickers hardness. The modulus decreased by 53% with the addition of 20 vol% h-BN, from 316 GPa for monolithic AlN to 148 GPa for specimens with 20 vol% hBN. Thus, the addition of BN resulted in a decrease in the modulus as well as an increase in the residual porosity, both of which contributed to the observed decrease in flexural strength and fracture toughness. Fig. 4 also shows a corresponding dramatic decrease in hardness, a decrease of about 85%.

The strength reduction may also be caused by the residual tensile stress developed by the difference in thermal expansion coefficient (TEC) between AlN and hBN. h-BN has an anisotropic TEC ($7.15 \times 10^{-6}\,C^{-1}$ along the *c*-axis and $0.77 \times 10^{-6}\,C^{-1}$ along the *a*-axis), but the TEC of AlN is isotropic ($5.6 \times 10^{-6}\,C^{-1}$).[4] The TEC mismatch between AlN and h-BN can lead to a residual tensile stress along the plane vertical to the *c*-axis of h-BN. Results of FEM analyses, to evaluate the residual stress, showed that a maximum tensile stress of about 130 MPa can be developed at the edge on a plane vertical to *c*-axis of h-BN.

According to the results of XRD analysis for AlN–hBN based composites. YAG ($Y_3Al_5O_{12}$) and γ-Al_2O_3 phases were detected in addition to major phases of AlN and h-BN. The YAG phase, located on triple points, was also conformed by TEM equipped with EDX. The occurrence of the YAG phase at the triple point was the consequence of the reaction ($3Y_2O_3 + 5Al_2O_3 \rightarrow 2Y_3Al_5O_{12}$) of the sintering aid, Y_2O_3, with Al_2O_3, which existed on the surface of AlN powders.[5] γ-Al_2O_3 phase could have been formed by the preferential loss of Y_2O_3 from YAG phase.[6]

Fig. 5 shows Vickers crack paths on AlN–hBN surfaces perpendicular to the direction of the uni-axial pressing. It can be seen that crack bridging and crack deflection seem to increase with the addition of hBN.

Because pressureless-sintered AlN–hBN composite has a texture structure, Vickers indentations with different directions were also made on the surface parallel to the direction of the uni-axial forming. Fig. 6 shows the changes of crack path with indentation angle. For the case of 0° angle (most of basal axes of BN particles are parallel to the indentation angle), the crack advanced in a relatively straight fashion along the interface of

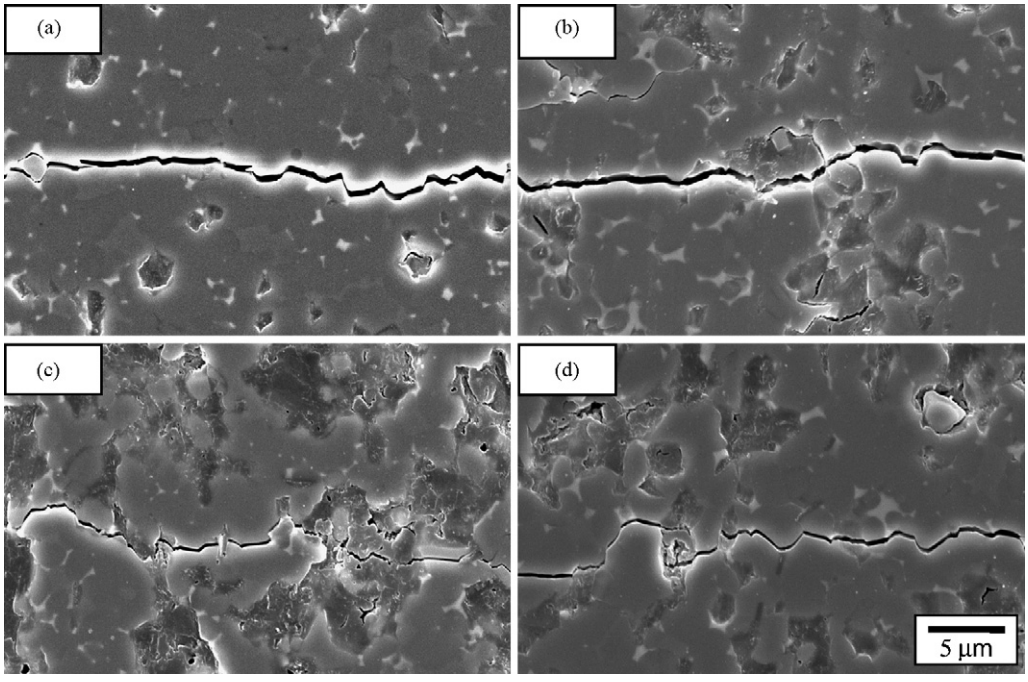

Fig. 5. Vickers crack propagation of AlN–hBN based composites on plane perpendicular to uni-axial pressing direction: (a) 0 vol% hBN, (b) 5 vol% hBN, (c) 10 vol% hBN, and (d) 15 vol% hBN.

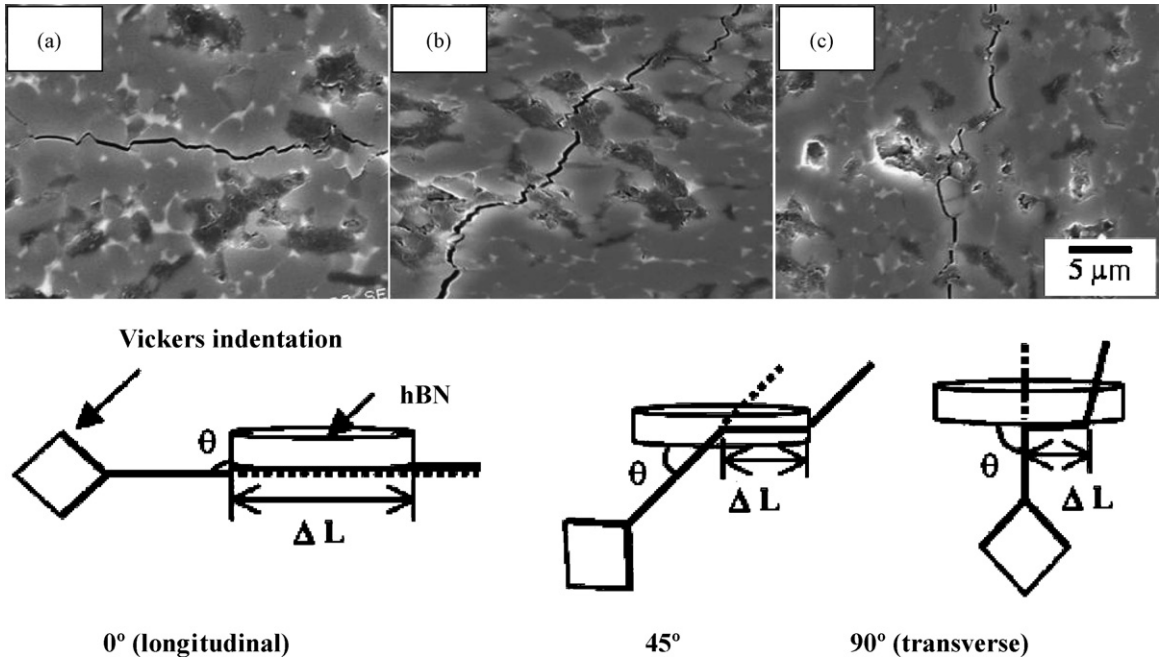

Fig. 6. Crack propagation of AlN–10 vol% hBN composites in plane parallel to uni-axial pressing direction. Vickers crack was introduced to (a) 0°, (b) 45°, and (c) 90°.

AlN–hBN. However, for the cases of the 45°, and 90° angles, the advancing crack is seen to be deflected by the h-BN grains.

Fig. 7 presents the cumulative length (the ratio of ΔL (refer to Fig. 6) to total crack length) as a function of the deflection angle.[7] The cumulated length of the deflected crack provides indirect information on the interfacial bond between the AlN matrix and h-BN. The lower location of curve, the weaker is the interfacial bond between the matrix and BN particles. Based on the results of Figs. 6 and 7, it was considered that AlN–BN composite had relatively weak interfacial bond between the matrix and BN particles.

Fig. 8 shows interaction between Vickers crack and hBN platelet on the surface parallel to the direction of the uni-axial forming pressure. It is clear that the crack advanced along the

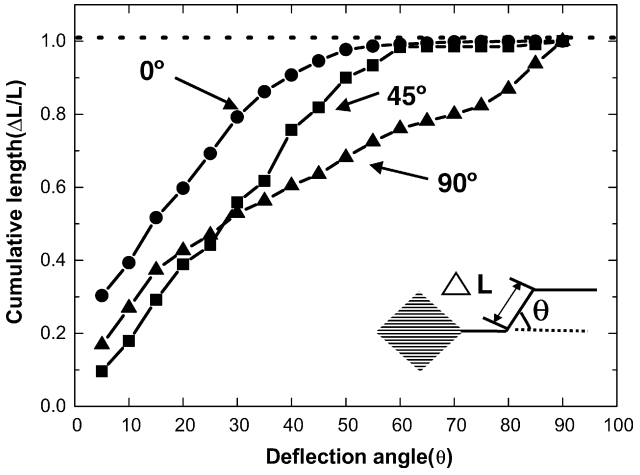

Fig. 7. Cumulative length of crack segment with deflected angle to main crack direction in plane parallel to uni-axial pressing direction for AlN–10 vol% hBN composite.

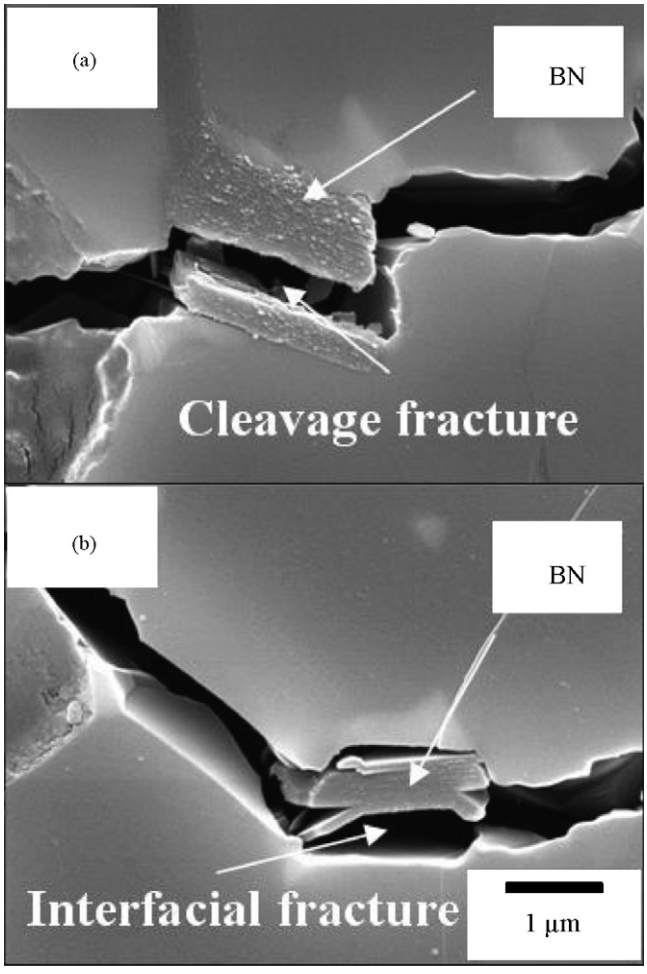

Fig. 8. Vickers crack interactions with hBN in AlN–10 vol% hBN composite. Vickers crack was made on plane parallel to uni-axial forming direction: (a) cleavage fracture, and (b) interfacial fracture.

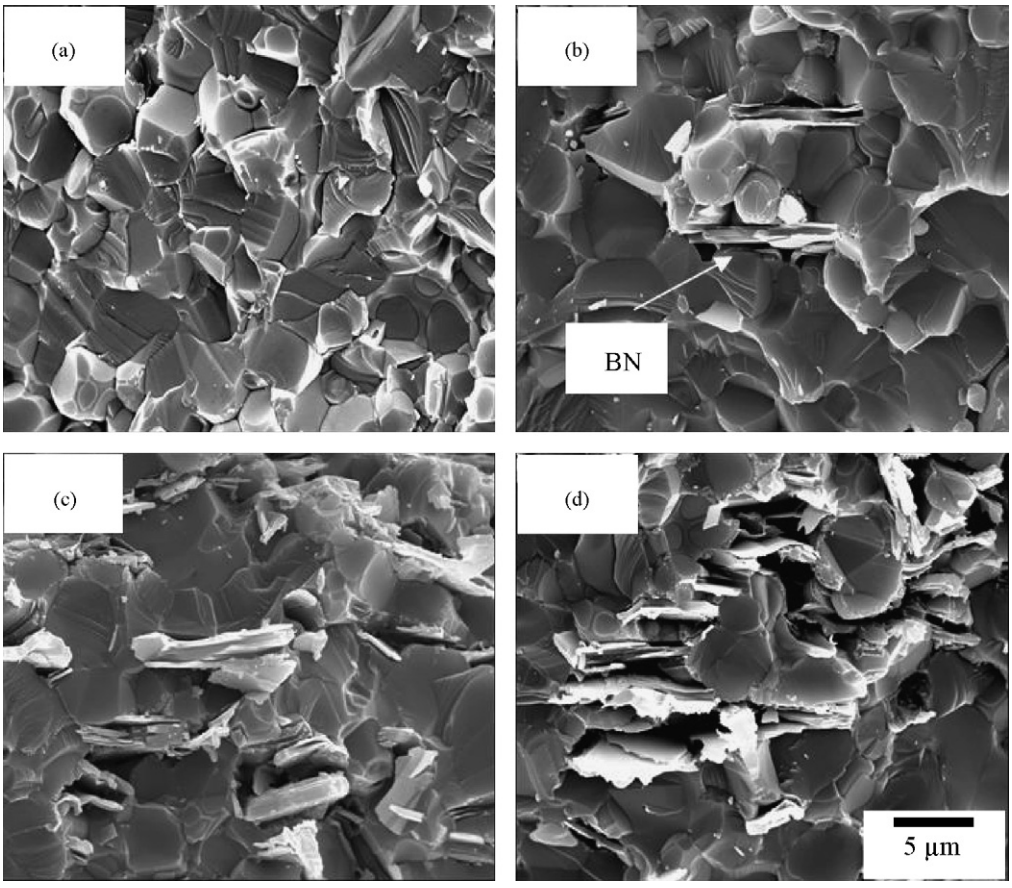

Fig. 9. The fracture surfaces of AlN–hBN based composites after four-point bending test: (a) 0 vol% hBN, (b) 5 vol% hBN, (c) 10 vol% hBN, and (d) 20 vol% hBN.

cleavage plane of hBN and interface of AlN–hBN. The interfacial fracture provides direct evidence for weak interfacial bond of AlN–hBN composites.

Fig. 9 shows examples of SEM micrographs of fracture surfaces after bending tests. AlN monolith (Fig. 9(a)) showed both intergranular and transgranular fractures, but AlN–hBN composites showed a higher tendency of transgranular fracture, a tendency which increased with increasing BN content. Residual pores were frequently observed in the vicinity of hBN platelets. Thus, the transition of the fracture mode, from intergranular to transgranular fracture, could be caused by increased residual pores, acting as fracture source. Based on the fracture surface observation, the reason of the decrease of flexural is mainly due to residual porosity: actually BN particles usually form pockets with density that ranges between 60 and 70%. Although increased residual pores deteriorated the strength of the composite, it is regarded to improve the resistance to thermal shock. Also, crack blunting effect by micropores existing in the advancing crack front can be expected. It would relieve the stress concentration and triaxial stress field developed around the crack tip,[8] thereby preventing the crack from propagating into the inner side of the composite.

In the case of AlN–BN composites, evidence for pull-outs of h-BN platelets was observed. Based on these microstructural observations, crack bridging and pull-out could be possible toughening mechanisms for AlN–BN composite.

As mentioned before, pressureless-sintered AlN–hBN composite exhibit strong texture of BN grains oriented with the *c*-axis parallel to the forming direction. This anisotropic texture might lead to rising crack resistance curve (*R*-curve)[9] by the bridging and pull-out of plate-like BN.

In this study, *R*-curve behaviors for the pressureless-sintered sample could not be characterized, since the effect of residual pores on the *R*-curve behavior is not simple to evaluate. Thus, based on our previous study on the AlN–BN composites,[10] we introduce here the *R*-curve behaviors of hot-pressed AlN–BN composites. The specimens were prepared by hot-pressing at 1800 °C for 2 h in N_2. The sintering temperature and holding time was identical as those for pressureless-sintered specimen. *R*-curves were obtained from the indentation strength data for the AlN–BN composites as compared with that of monolithic AlN. For the monolithic AlN, fracture toughness rose rapidly initially (at the relatively short crack lengths) but leveled off at higher crack lengths. The rapid rise of the fracture toughness is caused by the relatively small grain size in AlN. For the hot-pressed AlN–BN composites, the *R*-curve rises slowly with the initial fracture toughness being relatively low. But as the crack grew, fracture toughness increased and became higher than that of the monolithic AlN when the crack was longer than approximately 200 μm. A slowly rising *R*-curve behavior may be very important for the machinability of these composites. The toughness is low with small cracks, which enables easy machining

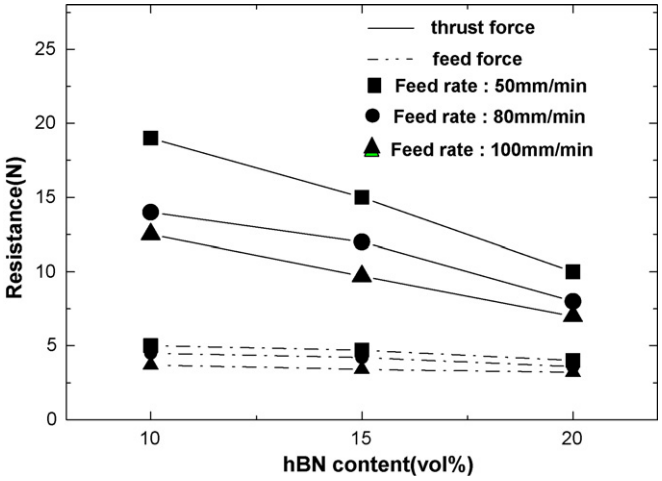

Fig. 10. Change of the thrust and feed force with hBN content. Cutting resistance was measured under the fixed feed rate of 50, 80, and 100 mm/min.

with a relatively low cutting force. However, the high toughness at long cracks prevents the cracks from propagating deeply to the inside of the composites, thereby minimizing machining damage.

Fig. 10 shows the cutting resistance as a function of hBN content. The cutting resistance of AlN monolith could not be measured due to its brittle fracture. The feed and thrust forces decreased with increasing h-BN content, showing excellent machinability. It is seen that the cutting resistance for the thrust force and the feed force became identical when the hBN content was 15 vol% or higher. During the microdrilling test, the resistance force also decreased from 2.0 to 0.5 N as cutting speed increased from 4000 to 6000 rpm.

4. Summary

The microstructure and mechanical properties of pressureless-sintered AlN–BN composites (with BN ranging from 0 to 20 vol%) were investigated with regards to their machinability. The results obtained can be summarized as follows:

1. Flexural strength, fracture toughness, hardness, and Young's modulus decreased with increasing h-BN content. For example, the flexural strength decreased from 340 MPa for monolith to 120 MPa by the addition of 20 vol% h-BN. The reason of the decrease of flexural strength is mainly due to the much higher residual porosity since BN particles usually form pockets with low density. In addition, the residual tensile stress, developed between AlN and the flat surface of h-BN, is a possible reason for the strength reduction.
2. The degree of crack deflection increased with an increase in the BN content. This was considered as an indication of the relatively weak interfacial bond between the AlN matrix and the BN particles. In AlN–BN composites, pull-outs of h-BN platelet were observed.
3. Fracture surface and indentation crack path studies showed that BN platelets induced grain pull-out and crack bridging during crack propagation. Crack bridging owing to the BN platelets in the composites should lead to a slowly rising *R*-curve behavior similar to that of the hot-pressed AlN–BN composites, which has been reported in another paper previously. The slowly rising *R*-curve may be very important for the excellent machinability of these composites.
4. During end-milling and microdrilling processes, feed and thrust forces decreased with increasing h-BN content, showing excellent machinability.

Acknowledgement

This work was supported by grant No. (R01-2001-000-00257-0) from the Basic Research Program of the Korean Science & Engineering Foundation.

References

1. Werdecker, W. and Aldinger, F., *IEEE Trans. Compon. Hybrids Manuf. Technol.*, 1984, **CHMT-7**, 399.
2. Blake, P., Bifano, T., Dow, T. and Scattergood, R. O., Precision machining of ceramic materials. *Am. Ceram. Soc. Bull.*, 1988, **67**, 1038–1043.
3. Funahashi, T. and Isomura, K., AlN composites ceramics. *Ceramics*, 1991, **26**, 749–753.
4. Shackerfold, J. F. and Alexander, W., *Materials science and engineering handbook* (*3rd ed.*). CRC Press, New York, 2001, p. 454.
5. Komeya, K., Inoue, H. and Tsuge, A., Effect of various additives on sintering of AlN. *J. Am. Ceram. Soc.*, 1981, **89**, 330–336.
6. Mitra, S., Dutta, G. and Dutta, I., Effect of heat treatment on the microstructure and properties of dense AlN sintered with Y_2O_3 additions. *J. Am. Ceram. Soc.*, 1995, **78**, 2335–2340.
7. Cho, W. S. and Hayashi, K., Effect of uni-directional orientation of SiC whiskers on mechanical properties of SiC whisker/Si_3N_4 composite ceramics. *J. Jpn. Inst. Metals*, 1992, **36**, 1087–1092.
8. Hertzberg, R. W., *Deformation and fracture mechanics of engineering materials*. John Wiley & Sons, New York, 1996, pp. 315–359.
9. Krause Jr., R. F., Rising fracture toughness from the bending strength of indented alumina beams. *J. Am. Ceram. Soc.*, 1988, **71**, 338–342.
10. Cho, W. S., Lee, Y. H., Cho, M. W., Lee, E. S., Lee, J. H., Hong, Y. C. *et al.*, Microstructure and mechanical properties of AlN–BN based machinable ceramics. *Key Eng. Mater.*, 2004, **264–268**, 873–876.